PHYSICAL REVIEW B VOLUME 31, NUMBER 5 1 MARCH 1985

ESR and susceptibility studies of stage-1 highly oriented pyrolytic graphite–OsF_6 graphite intercalation compound

D. Vaknin and D. Davidov*
Racah Institute of Physics, Hebrew University of Jerusalem, Jerusalem, Israel

H. Selig
Institute of Chemistry, Hebrew University of Jerusalem, Jerusalem, Israel

V. Zevin and I. Felner
Racah Insitute of Physics, Hebrew University of Jerusalem, Jerusalem, Israel

Y. Yeshurun
Physics Department, Bar-Ilan University, Ramat-Gan, Israel

(Received 20 August 1984; revised manuscript received 16 October 1984)

ESR and susceptibility studies of highly oriented pyrolytic graphite–OsF_6($C_{10}OsF_6$) stage-1 graphite intercalated compounds are reported. The anisotropy in both ESR and magnetization are interpreted in terms of a quartet ground state of Os^{+5}, $5d^3$ configuration, in axial local symmetry. The results yield information about charge transfer, anisotropic exchange, spin-orbit coupling, crystal-field splittings, and molecular orientation.

Bartlett, McCarron, McQuillan, and Thompson[1] have reported recently on the magnetic susceptibility of powdered samples of C_8OsF_6 graphite intercalated compound (GIC). Their results indicate Curie-Weiss behavior above $T=20$ K, but a significant deviation from a Curie-Weiss law below $T=20$ K. From their susceptibility data, Bartlett *et al.*[1] have concluded that the graphite-OsF_6 chemical reaction can be formulated as

$$nC + OsF_6 \rightarrow C_n^+ OsF_6^- \quad . \tag{1}$$

The present work uses the magnetic OsF_6^- intercalant ions ($5d^3$ configuration) as a probe to study the ESR and susceptibility of highly oriented pyrolytic graphite (HOPG)–OsF_6 with emphasis on stage-1 compounds.[2] Our results indicate large anisotropies in the magnetic properties which could not have been seen before in powdered samples. The data are analyzed using a crystal-field model and important information is obtained concerning the intercalant species, the local symmetry and orientation, as well as on the spin-spin anisotropic exchange.

The intercalation procedure was carried out as described by Bartlett.[1] A high-quality (001) x-ray diffraction pattern enables us to identify the stages.[1] The ESR was carried out in the X-band frequency range over the temperature range between 1 and 300 K. We use a finger-tip helium Dewar for measurements below 4 K but a Helitrans helium-flux system above 4 K. The susceptibility measurements were performed by using a vibrating-type magnetometer ($2\text{ K} < T < 300$ K) at the Hebrew University. Some measurements were performed also by using the superconducting quantum interference device (SQUID) at Bar-Ilan University down to $T=2$ K. The main results on stage-1 HOPG–OsF_6($C_{10}OsF_6$) can be summarized as follows.

The ESR spectra exhibit a single anisotropic line below $T=50$ K. The intensity of this line is roughly inversely proportional to the temperature, indicating Curie-like spins. Figure 1 exhibits the ESR spectra for various magnetic field orientations θ with respect to the $\vec{c}$ axis. As can be clearly seen the ESR lines exhibit Dysonian line shape[3] with A/B values of about 3–6 (the A/B ratio is defined by Feher and Kip[3]). The strong axial anisotropy of the ESR line could be expressed in terms of anisotropic effective g value as follows: $g_{\text{eff}}^2 = g_{\parallel}^2 \cos^2\theta + g_{\perp}^2 \sin^2\theta$, where θ measures the angle between the magnetic field $\vec{H}$ and the $\vec{c}$ axis of the HOPG slab. The parallel and perpendicular g factors are $g_{\parallel}=1.65\pm0.05$ and $g_{\perp}=3.25\pm0.05$. These g factors are temperature independent and no effects were observed using different methods of cooling such as field cooling or zero-field cooling. The ESR linewidth ΔH versus angle θ exhibits a shallow minimum around $\theta \simeq 60°$, approximately. The ESR linewidth increases almost linearly with increasing temperature. The thermal broadening b [$b=\delta(\Delta H)/\delta T$] was found to depend on sample orientation. Particularly, we found $b=9\pm2$ G/K for $\vec{H}$ parallel to the $\vec{c}$ axis ($\vec{H}\parallel\vec{c}$) and $b=6\pm1$ G/K for $\vec{H}$ perpendicular to the $\vec{c}$ axis

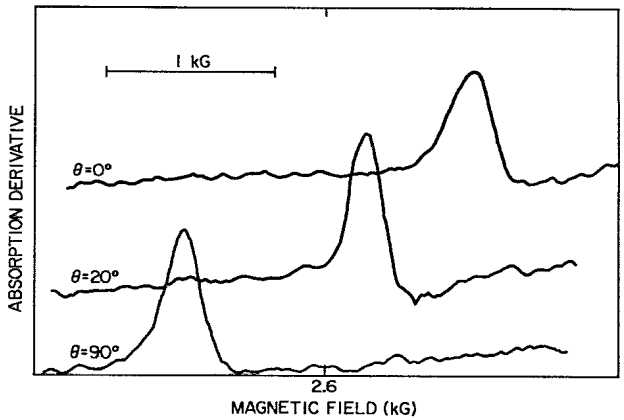

FIG. 1. ESR line shape of HOPG–OsF_6 ($C_{10}OsF_6$) stage 1 at $T=6$ K for various orientations θ. θ measures the angle between the magnetic field $\vec{H}$ and the $\vec{c}$ axis ($H_0=2600$ G; $\nu=9139$ MHz).

($\vec{H}\perp\vec{c}$) in the temperature range $1 < T < 30$ K. The observation of slight anisotropic thermal broadening might suggest anisotropic ion-conduction electron exchange interaction.[4]

The results described in Fig. 1 are for freshly prepared samples. We found, however, that the ESR linewidth broadens dramatically (by at least a factor of 3) for samples kept inside quartz tubing for a period of several months, although the spin density as extracted from susceptibility measurements almost does not change. These changes in the ESR linewidth are associated with dramatic broadening of the (001) x-ray diffraction spectra. We were not able to observe the free-carrier resonance (electrons and holes) in any of the C/OsF_6 GIC even for high stage samples.[5,6] Although the emphasis here is on stage-1 GIC, higher stages exhibit very similar ESR features.

The magnetization of HOPG–OsF_6 depends strongly on both temperature and sample orientation. It is almost isotropic at high temperatures but strongly anisotropic at low temperatures and independent of the method of cooling. The magnetization as a function of field strength at various temperatures (down to $T=2$ K) shows a linear behavior confirming the absence of magnetic order above $T=2$ K. The anisotropic magnetization yields an anistropic susceptibility. Figure 2 describes the inverse susceptibilities $1/\chi_\perp$ (circles) and $1/\chi_\parallel$ (triangles) for $\vec{H}\perp\vec{c}$ and $\vec{H}\parallel\vec{c}$, respectively. We note that $1/\chi_\perp$ versus temperature roughly exhibits a straight line. The longitudinal inverse susceptibility $1/\chi_\parallel$ exhibits a fast increase with increasing temperature at low T ($T<20$ K). At higher temperatures ($T>30$ K) both $\chi_\parallel$ and $\chi_\perp$ can be described in terms of a Curie-Weiss law: $\chi_\alpha = C/(T+\theta_\alpha)$ ($\alpha = \parallel, \perp$) with $\theta_\parallel \simeq 40$ K and $\theta_\perp \simeq 10$ K. Note also that at high temperatures the slopes of $1/\chi_\parallel$ and $1/\chi_\perp$ vs T are very similar, indicating an isotropic magnetic moment. Using $C = N\mu_{\rm eff}^2/3k_B$, we estimate an effective magnetic moment $\mu_{\rm eff} = 3.2\mu_B$ from the high-temperature data in Fig. 2.

Our experimental results above strongly suggest that the magnetic properties of HOPG–OsF_6 (stage 1) can be explained in terms of quartet ground state of the Os^{+5}, $5d^3$ configuration, in an axial symmetry (a slightly distorted octahedral crystal field). Such a configuration has been discussed extensively[7,8] in the past. The quartet is a result of admixture of a ground-state orbital singlet and excited triplet by the spin-orbit coupling.[7,8] The energy levels of this quartet can be described in terms of the following spin Hamiltonian with an effective spin $S=\frac{3}{2}$ ($2S+1=4$).

$$H = g\mu_B[H_zS_z + \tfrac{1}{2}(H_+S_- + H_-S_+)] + D[S_z^2 - \tfrac{1}{3}S(S+1)] \ , \tag{2}$$

where g and D are given in terms of the spin-orbit coupling λ and the singlet-triplet splitting Δ as[7,8]

$$g = 2(1-8\lambda/\Delta); \quad D = 4\lambda^2/\Delta \ . \tag{3}$$

Diagonalization of the 4×4 matrix associated with (2) yields the energy levels of the quartet. Particularly for $\vec{H}\parallel\vec{c}$, we find an exact solution

$$E^{(\pm1/2)} = -D \pm \tfrac{1}{2}g\mu_BH \ , \qquad E^{(\pm3/2)} = +D \pm \tfrac{3}{2}g\mu_BH \ . \tag{4}$$

For $\vec{H}\perp\vec{c}$ we find, in the first approximation ($g\mu_BH \ll 2D$)

$$E_\perp^{(\pm1/2)} = -D \pm g\mu_BH - \tfrac{3}{16}g^2\mu_B^2H^2/D \ , \qquad E_\perp^{(\pm3/2)} = +D + \tfrac{3}{16}g^2\mu_B^2H^2/D \ . \tag{5}$$

It is clearly seen from (4) and (5) that in zero field the quartet splits into two doublets ($\pm\frac{1}{2}$ and $\pm\frac{3}{2}$) with energy splitting of $2D$. The g values, $g_\parallel$ and $g_\perp$, of the ground-state doublet for ($\vec{H}\parallel\vec{c}$) and ($\vec{H}\perp\vec{c}$), respectively, can be extracted from the relation $g_\alpha = [E^{(1/2)} - E_\alpha^{(-1/2)}]/\mu_BH$, where $E_\alpha^{(\pm1/2)}$ are given by (4) and (5). We find $g_\parallel = g$ and $g_\perp \simeq 2g$. Thus, the spin Hamiltonian (2) correctly predicts the experimental ratio $g_\perp/g_\parallel \simeq 2$ as well as the angular dependence of the g value. The observation of a Curie-Weiss behavior at high temperatures indicates the importance of the spin-spin exchange interaction. We have modified, therefore, the spin Hamiltonian (2) to include Heisenberg-type exchange interaction in the molecular field approximation. We write

$$H_{\rm MF} = g\mu_B[(H_z+\lambda_\parallel M_\parallel)S_z + (H_x+\lambda_\perp M_x)S_x] + D[S_z^2 - \tfrac{1}{3}S(S+1)] \ , \tag{6}$$

where $\lambda_\parallel$ and $\lambda_\perp$ are related to the exchange parameters $J_\parallel$ and $J_\perp$, respectively, as follows:

$$\lambda_\parallel = J_\parallel/g^2\mu_B^2N; \quad \lambda_\perp = J_\perp/g^2\mu_B^2N \ . \tag{7}$$

In the molecular field approximation the susceptibility can be expressed as

$$\chi_\alpha = \chi_\alpha^{(0)}/(1-\lambda_\alpha\chi_\alpha^{(0)}) \quad (\alpha = \parallel, \perp) \ , \tag{8}$$

where $\chi_\alpha^{(0)}$ is the susceptibility in the absence of spin-spin exchange interaction. For $\chi_\alpha^{(0)}$ we write the standard formula[8]

$$\chi_\alpha^{(0)} = (N/ZH)\sum -(dE_\alpha^{(i)}/dH)\exp(-E_\alpha^{(i)}/k_BT) \ , \tag{9}$$

where the energy levels $E_\alpha^{(i)}$ ($\alpha = \parallel, \perp$) are given by Eqs. (4) or (5); Z is the partition function, N the Avogadro

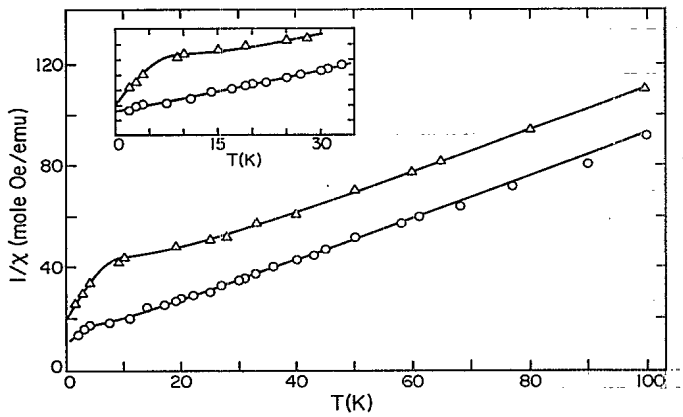

FIG. 2. Inverse longitudinal susceptibility, $1/\chi_\parallel$ (triangles), and the inverse transverse susceptibility $1/\chi_\perp$ (circles) vs temperatures. The solid line represents theoretical fit of our model to the experiment using the parameters $g=1.65$, $D=13$ K, $J_\parallel=-16$ K, $J_\perp=-12$ K. The inset: the fit at low temperatures.

number, and k_B the Boltzman factor. At the high-temperature limit ($k_BT \gg D$, $g\mu_BH$) the susceptibility (8) can be written as a Curie-Weiss $\chi_\alpha = C/(T+\theta_\alpha)$, where $C = g^2\mu_B^2 NS(S+1)/3k_B$ and θ_α are given by

$$\theta_\parallel = -C\lambda_\parallel + \tfrac{4}{5}D = -\tfrac{5}{4}J_\parallel + \tfrac{4}{5}D \ ,$$
$$\theta_\perp = -C\lambda_\perp - \tfrac{2}{5}D = -\tfrac{5}{4}J_\perp - \tfrac{2}{5}D \ . \qquad (10)$$

It is seen that the θ_α depend on both the exchange parameters and the crystalline field splitting. The solid line in Fig. 2 represents a reasonable fit of our model, Eqs. (8) and (9), to the experimental susceptibilities. In the fitting procedure we have used the value of $g = 1.65$ from the ESR data and have searched for the best unknown parameters D, $J_\parallel$, and $J_\perp$. Our best fit yields $D = 13$ K, $J_\parallel = -16$ K, $J_\perp = -12$ K. Knowledge of $D = 13$ K and $g = 1.65$ enables one to estimate the spin-orbit coupling λ and the singlet-triplet splitting Δ using (3). We find $\lambda = 149$ K and $\Delta = 6792$ K. Note, also, that at high temperatures the isotropic magnetic moment is given by $\mu_{\text{eff}} = g\mu_B\sqrt{S(S+1)}$. Using $g = 1.65$ and $S = \frac{3}{2}$, we find a theoretical value for the magnetic moment: $\mu_{\text{eff}} = 3.2\mu_B$. This is in excellent agreement with experiment. Using (10) together with $J_\parallel = -16$ K and $J_\perp = -12$ K the Curie-Weiss temperatures are found to be $\theta_\parallel = +31$ K and $\theta_\perp = 10$ K, in good agreement with experiment.

The observation of relatively large exchange parameters but the absence of magnetic ordering down to 2 K is a remarkable feature. HOPG–OsF_6 is, thus, different from other magnetic GIC such as HOPG–$FeCl_3$, HOPG–$CoCl_3$, HOPG–$NiCl_2$, and HOPG–$CoCl_2$, which exhibit magnetic order.[9] It should be noted that in all these magnetic GIC the pristine intercalant species are magnetic and retain this property in the intercalation compound. HOPG–OsF_6 is prepared from the gas phase of OsF_6 and its magnetic properties are due to the charge transfer [Eq. (1)], i.e., there is no correlation with the magnetic properties of the starting materials.

Following are our conclusions.

(1) The combined experiments provide evidence that the intercalant species are almost completely in the form of OsF_6^-. The prediction of Bartlett *et al.* is correct:[1] There is a charge transfer of one electron per each OsF_6 formula. Previous studies of GIC with fluorides such as HOPG–AsF_5 have shown significantly smaller charge transfer per molecule.[10] This is probably associated with the fact that the chemical reaction does not always go to completion in some of these GIC fluorides.

(2) The experimental results indicate the existence of a well-defined crystal field and a well-defined orientation of the intercalant species. The suggestion of Bartlett *et al.*[1] that the C_3 axis of the OsF_6^- ion is parallel to the $\vec{c}$ axis (see Fig. 5 in Ref. 1) is consistent with our observation for freshly prepared samples.

(3) The susceptibility study provides evidence for anisotropic antiferromagnetic spin-spin exchange interaction. The crystallographic studies of Bartlett *et al.*[1] on C_8OsF_6 indicate an hexagonal structure with unit cell dimensions of $a \sim 4.9$ Å and $c \sim 8.1$ Å.[1] For a single OsF_6^- molecule per unit cell in stage-1 compounds, the in-plane distance between OsF_6^- molecules is significantly shorter than this distance along the c axis. This might suggest that the exchange parameters $J_\parallel$ and $J_\perp$ are dominated by in-plane interactions.

(4) The absence of long-range magnetic order down to 2 K for relatively large in-plane Heisenberg exchange parameters ($J_\parallel = -16$ K, $J_\perp = -12$ K) might suggest that HOPG–OsF_6 is truly two-dimensional magnet and the long-range magnetism is destroyed by fluctuations, according to the classical Mermin-Wagner theorem.[11] We are currently conducting measurements on higher stages to check critically if indeed HOPG–OsF_6 is a realization of two-dimensional magnetic system according to the Mermin-Wagner theorem.

The authors wish to thank Dr. Moore of Union Carbide for providing the HOPG. This work was supported by Stiftung Volkswagenwerk.

---

*Present address: Physics Department, University of California at Santa Barbara, Santa Barbara, California 93106.

[1]N. Bartlett, E. M. McCarron, B. W. McQuillan, and T. E. Thompson, Synth. Met. **1**, 221 (1979/1980).

[2]A preliminary report on this work was given at the 8th European Symposium on Fluorine Chemistry, Jerusalem, Israel, August, 1983. See D. Vaknin, D. Davidov, Y. Yeshurun, and H. Selig, J. Fluor. Chem. **23**, 425 (1983).

[3]G. Feher and A. F. Kip, Phys. Rev. **98**, 377 (1955).

[4]D. Vaknin (unpublished).

[5]S. K. Khanna, E. R. Falardeau, A. J. Heeger, and J. E. Fischer, Solid State Commun. **25**, 1059 (1978); O. Milo, Master's thesis, Jerusalem, 1984 (unpublished).

[6]D. Davidov, O. Milo, I. Palchan, and H. Selig, Synth. Met. **8**, 83 (1983).

[7]A. Abragam and B. Bleany, *Electron Paramagnetic Resonance of Transition Ions* (Clarendon, Oxford, 1970), pp. 126–127, and references therein.

[8]C. J. Ballhausen, *Introduction to Ligand Field Theory* (McGraw-Hill, New York, 1962), pp. 279–281.

[9]See, for example, M. Suzuki *et al.*, Synth. Met. **8**, 43 (1983); C. H. Simon *et al.*, *ibid.* **8**, 53 (1983); H. Suematsu *et al.*, *ibid.* **8**, 23 (1983); M. Elahy *et al.*, *ibid.* **8**, 35 (1983).

[10]H. Selig (unpublished); J. E. Fischer, A. Metrot, P. J. Flanders, W. R. Salaneck, and C. F. Brucker, Phys. Rev. B **23**, 5576 (1981); M. S. Dresselhaus and G. Dresselhaus, Adv. Phys. **30**, 139 (1981).

[11]N. D. Mermin and H. Wagner, Phys. Rev. Lett. **17**, 1133 (1966).